REVISION 2

Densified glasses as structural proxies for high-pressure melts: configurational compressibility of silicate melts retained in quenched and decompressed glasses

Wim J. Malfait [1,2*], Rita Seifert [1] and Carmen Sanchez-Valle [1]

[1] *Institute of Geochemistry and Petrology, ETH Zurich, Switzerland*

[2] *Laboratory for Building Science and Technology, EMPA Dübendorf, Switzerland*

[*]Corresponding authors. Address: Laboratory for Building Science and Technology, EMPA, Überlandstrasse 129, 8600 Dübendorf, Switzerland. E-mail address: wim.malfait@empa.ch.

ABSTRACT

The structures of high-pressure magmatic liquids have often been inferred from spectroscopic studies on quenched and decompressed glasses. However, it has not been completely verified whether the structures of quenched and decompressed glasses are representative of the structure of their corresponding liquids at the glass transition temperature and synthesis pressure. Here, we provide quantitative evidence for the retention of pressure-induced configurational changes upon isobaric quench and isothermal decompression for synthesis pressures up to 3.5 GPa. We use the degree of densification and elastic compressibility of permanently densified glasses, together with thermo-elastic data from the literature, to calculate the density of the melt at the glass transition temperature and synthesis pressure. The derived densities agree with those derived directly from the thermal equations of state of the

melts. This observation indicates that, at least up to 3.5 GPa, the densified structure of the melt is preserved in the glass upon quenching and decompression; this validates past and future structural studies of high-pressure melts based on studies of quenched and decompressed glasses.

Keywords: configurational compressibility, elastic compressibility, high pressure, silicate melts, density, relaxation, rhyolite, phonolite, basalt

INTRODUCTION

The structure of high-pressure magmatic liquids has often been inferred from spectroscopic and diffraction studies on quenched and decompressed glasses (Allwardt et al. 2005a, 2005b, 2007; Davoli et al. 1992; Du et al. 2004; Fleet et al. 1984; Fuss et al. 2006; Gaudio et al. 2008; Hochella and Brown 1985; Kelsey et al. 2009a, 2009b; Lee 2004, 2010, 2011; Lee et al. 2004, 2012; Li et al. 1995; Malfait et al. 2012; O'Neill et al. 2006; Paris et al. 1994; Stebbins and McMillan 1989; Stebbins and Poe 1999; Stebbins and Sykes 1990; Sykes et al. 1993; Velde and Kushiro 1978; Xue et al. 1989, 1991, 1994; Yamada et al. 2010; Yarger et al. 1995). The main advantage of using quenched glasses is that more numerous and more informative structural probes are available at ambient conditions than at *in situ* high pressure and temperature conditions. However, pressure-induced structural changes are not necessarily retained upon decompression, and studies on quenched and decompressed glasses may underestimate the effect of pressure on melt structure (Farber and Williams 1996; Shim and Catalli 2009). Until now, it has not been fully tested how representative the structures of quenched and decompressed glasses are of the structures of the corresponding melts.

Glasses differ fundamentally from melts. Liquids and glasses are commonly described in terms of equilibrium (relaxed) and non-equilibrium (unrelaxed) states, respectively (Dingwell and Webb 1990; Moynihan et al. 1976). The short lifetimes of the Si-O bonds allow for rapid re-equilibration in liquid silicates, but are too long for re-equilibration in the glassy state (Farnan and Stebbins 1990,1994; Malfait and Halter 2008). The glass transition temperature, T_g, the boundary between the liquid and glassy states, defines the temperature at which the structure is frozen in because the material is no longer able to re-equilibrate to the change in temperature during cooling. This transition typically occurs over a few tens of degrees (Mysen and Richet 2005). The temperature for which the frozen structure corresponds to the equilibrium state is called the fictive temperature, T_f (Moynihan et al. 1976; Tool 1946). Experimental studies on quenched glasses, combined with in situ studies of the corresponding liquids, have confirmed that the structure of the glass is indeed representative of the melt at the fictive temperature, at least with respect to the Al coordination number (Stebbins et al. 2008), water speciation (Behrens and Nowak 2003) and silica speciation (Brandriss and Stebbins 1988; Malfait et al. 2008; McMillan et al. 1992; Mysen and Frantz 1994).

Liquids and glasses also show notable differences in the compression mechanisms, with both elastic and configurational compression in liquids, but only elastic compression in glasses (Dingwell and Webb 1990). As a result, liquids are more compressible than their analog glasses. Richet and Neuville (1992) reported that the greater compressibility of liquids reflects configurational contributions. In other words, liquids are more compressible because a large number of densified configurational states are available through pressure-induced structural changes. For a frozen structure, the effects of pressure are elastic only and mostly related to variations in the interatomic bond lengths (Richet and Neuville 1992). The relative importance of the vibrational and configurational contributions to the compressibility depends

strongly on melt composition and structure (Askarpour et al. 1993). When a glass that was isobarically quenched from the liquid is decompressed to ambient pressure, the elastic contribution to the compressibility is released, but the configurational contribution is at least partially retained (Maurer 1957). However, the degree to which the configurational compression is retained upon decompression has not been quantified. Thus, it is not clear in how far the structure of quenched and decompressed glasses is representative of that of the melt at synthesis pressure.

The distinction between glass- and melt-like compressional behaviors becomes blurred when glasses are compressed to very high pressures. Indeed, glasses compressed to lower mantle pressures often display pressure-induced structural changes (Benmore et al. 2010; Champagnon et al. 2008; Hemley et al. 1986; Kubicki et al. 1992; Lee et al. 2008; Lin et al. 2007; Meade et al. 1992; Sato and Funamori 2008; Shim and Catalli 2009; Williams and Jeanloz 1988) and some irreversible, hence non-elastic, densification (Champagnon et al. 2008; Gaudio et al. 2008; Sanchez-Valle and Bass 2010; Zha et al. 1994).

In this study, we demonstrate that quenched and decompressed glasses represent the structure of the melt at high pressure and T_g, at least for subduction zone conditions. In particular, we use the degree of densification and elastic compressibility of permanently densified glasses, together with thermo-elastic data from the literature, to calculate the density of the melt at T_g and synthesis pressure. Within uncertainty, the obtained densities agree with those derived from the equations of state of the corresponding melts. This observation implies that the configurational compressibility is fully retained upon decompression for synthesis pressures up to at least 3.5 GPa.

DATA SOURCE

Three glass compositions were considered in this study: haplo-rhyolitic, haplo-phonolitic and haplo-basaltic. All samples are part of a set of well-characterized samples prepared for a previous study on the partial molar properties of dissolved CO_2, and a full description of their synthesis and characterization can be found there (Seifert et al. 2013a). For the current study, only the data for the CO_2-free glasses are considered. Briefly, permanently densified glasses were synthesized from 2 to 3.5 GPa and 1400-1750 °C in a piston cylinder apparatus using Pt capsules and a talc-MgO-silica assembly. The samples were quenched with an estimated quench rate of 100-200 K/s and decompressed at a rate of ~10 MPa/s. The major element composition and volatile contents were analyzed by electron microprobe and by Fourier transform infrared spectroscopy (FTIR), respectively (Table 1). The density of the glasses was determined with the sink/float method in a diiodomethane (CH_2I_2)-acetone (C_3H_6O) mixture. Relaxation experiments were performed on a fraction of each sample in order to remove the residual densification of the samples synthesized at high pressure. In this process, the samples undergo a structural reconfiguration by annealing them at ambient pressure near T_g, at 898, 879 and 913 K for the basaltic, phonolitic and rhyolitic glasses, respectively (Seifert et al. 2013a). Microscopic observation with crossed polarizers indicated that the annealed samples were free of crystals. Brillouin scattering spectroscopy has been used to measure the acoustic velocities and to derive the elastic properties of both permanently densified and relaxed glasses (Table 2) (Seifert et al. 2013a). All measurements were carried out in a 90° symmetric/platelet scattering geometry using the experimental setup described in Sanchez-Valle et al. (2010). The acoustic velocities were employed to calculate the adiabatic bulk modulus, *K*s, of each sample using the relationship:

$$K_S = \rho\left(v_P^2 - \frac{4}{3}v_S^2\right) \quad (1)$$

where ρ is the density, v_P and v_S are the compressional and shear wave velocities, respectively.

RESULTS & DISCUSSION

The density of the melt at the synthesis pressure and T_g (Giordano et al. 2008) was calculated based on the properties of the quenched glasses (Table 2) and the results compared with the density predicted by *in situ* measurements conducted in the corresponding haplo-ryholitic and haplo-phonolitic melts (Malfait et al. 2014; Seifert et al. 2013b). No in situ data are available for this particular haplo-basaltic glass composition, and the density of the melt, calculated from the quenched glasses, was compared to that predicted by a multi-component model for silicate melt density. This model predicts melt density based on the available density and compressibility data at ambient pressure and *in situ* density data for a range of melt compositions (Malfait et al., (subm.)).

The procedure to calculate the density of the high-pressure melt from the data on the ambient pressure glasses is illustrated in Figure 1. The configurational contribution to the pressure-induced densification of melts ($\beta_{configurational}$), $\Delta(\rho_0-\rho_1)$, was determined from density measurements on relaxed (ρ_0) and permanently densified (ρ_1) glasses. The elastic contribution ($\beta_{elastic}$), $\Delta(\rho_2-\rho_1)$, was calculated from K_S determined by Brillouin scattering data and a 3rd-order Birch-Murnaghan equation of state. In the absence of data for the pressure derivatives of the bulk modulus, K', of the investigated glasses, calculations of the elastic compressibility were performed for K' values of 2, 4, 6 and 8. The lower bound of this range was selected based on results from high-pressure Brillouin studies on glasses with soda-lime or enstatite (K'= 2.7±0.1) compositions that show a relatively small increase of K_s upon compression up to 5-8 GPa (Sanchez-Valle and Bass 2010; Tkachev et al. 2005). The upper bound was set

153 based on values obtained from compressibility data on liquids (Malfait et al. 2014; Sakamaki
154 et al. 2010; Seifert et al. 2013b). The possible variation of K' between 2 and 8 was found to
155 affect the calculated densities by less than 0.6, 0.2 and 0.3 % for the rhyolitic, phonolitic and
156 basaltic glasses, respectively. This variation was included in the uncertainty calculation on ρ_2.
157 The small dependence of the calculated densities on K' is related to the rather limited range of
158 compression of the present study (Table 2). In the last step, the temperature dependence of the
159 density, $\Delta(\rho_2-\rho_3)$, was estimated from the ambient pressure thermal expansion coefficient, α
160 (Bouhifd et al. 2001; Ochs and Lange 1999; Richter and Simmons 1974). This step assumes
161 that the temperature dependence of α is not significant, consistent with the small pressure-
162 temperature cross terms in the equations of state of silicate melts (Malfait et al. 2014;
163 Sakamaki et al. 2010; Seifert et al. 2013b).
164
165 The derived densities for the high-pressure melt at T_g, ρ_3, appear to be slightly lower
166 than those predicted by the equations of state of the analog melts, ρ_4, but are the same within
167 the estimated uncertainties (Table 2, Fig. 1). This implies that, within uncertainty, the
168 configurational compression is fully retained in the glasses during the isobaric quench and
169 isothermal decompression at the end of the piston cylinder experiments. Thus, no significant
170 configurational changes occurred during decompression. Hence, the glasses quantitatively
171 probe the configurations of the melt at the synthesis pressure and T_g, at least for the
172 investigated pressure range up to 3.5 GPa, and structural studies on quenched glasses can
173 provide valuable insights into the structure of high pressure melts at crustal and subduction
174 zone conditions.
175
176 There are some indications that some of the configurational changes during
177 compression may not be fully retained during decompression from higher pressures than those
178 investigated in this study. For example, the degree of densification and Al coordination

number decrease with decreasing decompression rate for glasses quenched and decompressed from 5 GPa, although the changes are relatively small: V/V_0 increases from 0.88 to 0.90 and the average Al coordination decreases from 4.95 to 4.75 for a decrease in decompression rate by over four orders of magnitude (Allwardt et al. 2005b). In addition, cold-compressed glasses display partly reversible pressure-induced structural changes (Hemley et al. 1986; Lin et al. 2007; Williams and Jeanloz 1988), although annealing glasses at high pressure makes the densification less reversible (Gaudio et al. 2008) and quenching from the melt at high pressure, rather than after cold compression of the glass, may result in a better retention of the pressure induced densification.

In summary, we provide quantitative evidence for the preservation of the pressure-induced densification and configurations of silicate melts upon quenching and decompression from subduction zone pressures. This observation validates past and future structural studies of high pressure melts based on quenched and decompressed glasses, for which more, and often more informative, analytical techniques are available, compared to liquids that require challenging *in situ* measurements.

ACKNOWLEDGEMENTS

We would like to thank Sung Keun Lee and two anonymous reviewers for their comments that substantially improved this manuscript and Ian Swainson for efficient editorial handling. This work was supported by the Swiss National Science Foundation (200020_140558 to CSV).

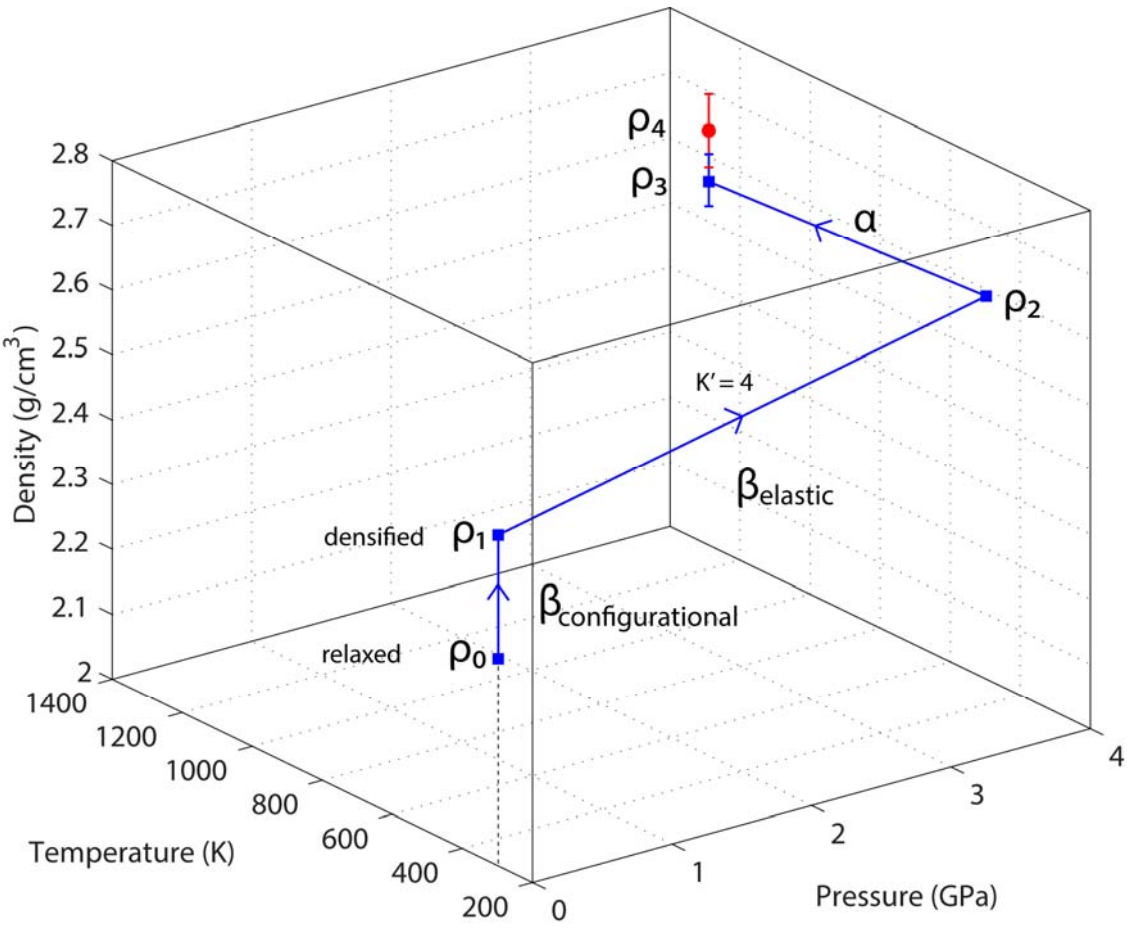

Fig. 1. Elastic and configurational contributions to the compression of rhyolitic glasses and melts. ρ_3 is the density of the melt at T_g and synthesis pressure (3.5 GPa) calculated from thermo-elastic data for glasses measured at ambient conditions: the configurational compression is estimated from the permanent densification (ρ_1-ρ_0); the elastic compression (ρ_2-ρ_1) from Brillouin scattering on densified glasses (Seifert et al. 2013a) and a 3rd order Birch-Murnaghan equation of state; and the thermal expansion (ρ_3-ρ_2) from the literature (Ochs and Lange 1999). ρ_4 is the density derived from the equation of state of the melt at T_g (Malfait et al. 2014). Within uncertainty, ρ_3 and ρ_4 are the same, implying that the configurational compressibility of silicate liquids is preserved upon quenching and decompression.

REFERENCES

Allwardt, J.R., Poe, B.T., and Stebbins, J.F. (2005a) The effect of fictive temperature on Al coordination in high-pressure (10 GPa) sodium aluminosilicate glasses. American Mineralogist, 90, 1453-1457.

Allwardt, J.R., Stebbins, J.F., Schmidt, B.C., Frost, D.J., Withers, A.C., and Hirschmann, M.M. (2005b) Aluminum coordination and the densification of high-pressure aluminosilicate glasses. American Mineralogist, 90, 1218-1222.

Allwardt, J.R., Stebbins, J.F., Terasaki, H., Du, L.S., Frost, D.J., Withers, A.C., Hirschmann, M.M., Suzuki, A., and Ohtani, E. (2007) Effect of structural transitions on properties of high-pressure silicate melts: ^{27}Al NMR, glass densities, and melt viscosity. American Mineralogist, 92, 1093-1104.

Askarpour, V., Manghnani, M.H., and Richet, P. (1993) Elastic Properties of Diopside, Anorthite, and Grossular Glasses and Liquids - a Brillouin-Scattering Study up to 1400 K. Journal of Geophysical Research-Solid Earth, 98, 17683-17689.

Behrens, H., and Nowak, M. (2003) Quantification of H_2O speciation in silicate glasses and melts by IR spectroscopy - In situ versus quench techniques. Phase Transitions, 76, 45-61.

Benmore, C.J., Soignard, E., Amin, S.A., Guthrie, M., Shastri, S.D., Lee, P.L., and Yarger, J.L. (2010) Structural and topological changes in silica glass at pressure. Physical Review B 81, 054105.

Bouhifd, M.A., Whittington, A., and Richet, P. (2001) Partial molar volume of water in phonolitic glasses and liquids. Contributions to Mineralogy and Petrology, 142, 235-243.

Brandriss, M.E., and Stebbins, J.F. (1988) Effects of temperature on the structures of silicate liquids: ^{29}Si NMR results. Geochimica et Cosmochimica Acta, 52, 2659-2669.

Champagnon, B., Martinet, C., Boudeulle, M., Vouagner, D., Coussa, C., Deschamps, T., and Grosvalet, L. (2008) High pressure elastic and plastic deformations of silica: in situ diamond anvil cell Raman experiments. Journal of Non-Crystalline Solids, 354, 569-573.

Davoli, I., Paris, E., Stizza, S., Benfatto, M., Fanfoni, M., Gargano, A., Bianconi, A., and Seifert, F. (1992) Structure of densified vitreous silica: silicon and oxygen XANES spectra and multiple scattering calculations. Physics and Chemistry of Minerals, 19, 171-175.

Dingwell, D.B., and Webb, S.L. (1990) Relaxation in silicate melts. European Journal of Mineralogy, 2, 427-449.

Du, L.S., Allwardt, J.R., Schmidt, B.C., and Stebbins, J.F. (2004) Pressure-induced structural changes in a borosilicate glass-forming liquid: boron coordination, non-bridging oxygens, and network ordering. Journal of Non-Crystalline Solids, 337, 196-200.

Farber, D.L., and Williams, Q. (1996) An in situ Raman spectroscopic study of $Na_2Si_2O_5$ at high pressures and temperatures: structures of compressed liquids and glasses. American Mineralogist, 81, 273-283.

Farnan, I., and Stebbins, J.F. (1990) Observation of slow atomic motions close to the glass transition using 2-D ^{29}Si NMR. Journal of Non-Crystalline Solids, 124, 207-215.

Farnan, I., and Stebbins, J.F. (1994) The nature of the glass transition in a silica-rich oxide melt. Science, 265, 1206-1209.

Fleet, M., Herzberg, C.T., Henderson, G.S., Crozier, E.D., Osborne, M.D., and Scarfe, C.M. (1984) Coordination of Fe, Ga and Ge in high pressure glasses by Mössbauer, Raman and X-ray absorption spectroscopy, and geological implications. Geochimica et Cosmochimica Acta, 48, 1455-1466.

Fuss, T., Mogus-Milankovic, A., Ray, C.S., Lesher, C.E., Youngman, R., and Day, D.E. (2006) Ex situ XRD, TEM, IR, Raman and NMR spectroscopy of crystallization of lithium disilicate glass at high pressure. Journal of Non-Crystalline Solids, 352, 38-39.

Gaudio, S.J., Sen, S., and Lesher, C.E. (2008) Pressure-induced structural changes and densification of vitreous $MgSiO_3$. Geochimica et Cosmochimica Acta, 72, 1222-1230.

Giordano, D., Russel, J.K., and Dingwell, D.B. (2008) Viscosity of magmatic liquids: a model. Earth and Planetary Science Letters, 271, 123-134.

Hemley, R.J., Mao, H.K., Bell, P.M., and Mysen, B.O. (1986) Raman spectroscopy of SiO_2 glasses at high pressure. Physical Review Letters, 57, 747-750.

Hochella, M.F., and Brown, G.E. (1985) The structures of albite and jadeite composition glasses quenched from high pressure. Geochimica et Cosmochimica Acta, 49, 1137-1142.

Kelsey, K.E., Stebbins, J.F., Mosenfelder, J.D., and Asimow, P.D. (2009a) Simultaneous aluminum, silicon, and sodium coordination changes in 6 GPa sodium aluminosilicate glasses. American Mineralogist, 94, 1205-1215.

Kelsey, K.E., Stebbins, J.F., Singer, D.M., Brown, G.E., Mosenfelder, J.D., and Asimow, P.D. (2009b) Cation field strength effects on high pressure aluminosilicate glass structure: multinuclear NMR and La XAFS results. Geochimica et Cosmochimica Acta, 73, 3914-3933.

Kubicki, J.D., Hemley, R.J., and Hofmeister, A.M. (1992) Raman and infrared study of pressure-induced structural changes in $MgSiO_3$, $CaMgSi_2O_6$ and $CaSiO_3$ glasses. American Mineralogist, 77, 258-269.

Lee, S.K. (2004) Structure of silicate glasses and melts at high pressure: quantum chemical calculations and solid-state NMR. Journal of Physical Chemistry B, 108, 5889-5900.

Lee, S.K. (2010) Effect of pressure on structure of oxide glasses at high pressure: insights from solid-state NMR of quadrupolar nuclides. Solid State Nuclear Magnetic Resonance, 38, 45-57.

Lee, S.K. (2011) Simplicity in melt densification in multicomponent magmatic reservoirs in Earth's interior revealed by multinuclear magnetic resonance. Proceedings of the National Academy of Science, 108, 6847-6852.

Lee, S.K., Cody, G.D., Fei, Y., and Mysen, B.O. (2004) Nature of polymerization and properties of silicate melts and glasses at high pressure. Geochimica et Cosmochimica Acta, 68, 4189-4200.

Lee, S.K., Lin, J.F., Cai, Y.Q., Hiraoka, N., Eng, P., Okuchi, T., Mao, H.K., Meng, Y., Hu, M.Y., Chow, P., Shu, J., Li, B., Fukui, H., Lee, B.H., Kim, H.N., and Yoo, C.S. (2008) X-ray Raman scattering study of $MgSiO_3$ glass at high pressure: implication for triclustered $MgSiO_3$ melt in Earth's mantle. . Proceedings of the National Academy of Science, 105, 7925-7929.

Lee, S.K., Yi, Y.S., Cody, G.D., Mibe, K., Fei, Y., and Mysen, B.O. (2012) Effect of network polymerization on the pressure-induced structural changes in sodium aluminosilicate glasses and melts: ^{27}Al and ^{17}O solid-state NMR study. Journal of Physical Chemistry C, 116, 2183-2191.

Li, D., Secco, R.A., Bancroft, G.M., and Fleet, M.E. (1995) Pressure-induced coordination change of Al in silicate melts from Al K-edge Xanes of high pressure $NaAlSi_2O_6$-$NaAlSi_3O_8$ glasses. Geophysical Research Letters, 22, 3111-3114.

Lin, J.F., Fukui, H., Prendergast, D., Okuchi, T., Cai, Y.Q., Hiraoka, N., Yoo, C.S., Trave, A., Eng, P., Hu, M.Y. and Chow, P. (2007) Electronic bonding transition in compressed SiO_2 glass. Physical Review B, 75, 012201.

Malfait, W.J., and Halter, W. (2008) Structural relaxation in silicate glasses and melts: results from high-temperature Raman spectroscopy and implications for bulk melt properties. Physical Review B, 77, 014201.

Malfait, W.J., Zakaznova-Herzog, V.P., and Halter, W.E. (2008) Quantitative Raman spectroscopy: speciation of Na-silicate glasses and melts. American Mineralogist, 93, 1505-1518.

Malfait, W.J., Verel, R., Ardia, P., and Sanchez-Valle, C. (2012) Aluminium coordination in rhyolite and andesite glasses and melts: effect of temperature, pressure, composition and water content. Geochimica et Cosmochimica Acta, 77, 11-26.

Malfait, W.J., Seifert, R., Petitgirard, S., Perrillat, J.-P., Mezouar, M., Ota, T., Nakamura, E., Lerch, P., and Sanchez-Valle, C. (2014) Supervolcano eruptions driven by melt buoyancy in large silicic magma chambers. Nature Geoscience, 7, 122-125.

Malfait, W.J., Seifert, R., and Sanchez-Valle, C. ((subm.)) A model for the density of volatile-bearing silicate melts at crustal and upper mantle conditions based on high-pressure experimental data. Earth and Planetary Science Letters.

Maurer, R.D. (1957) Pressure Effects in the Transformation Range of Glass. Journal of the American Ceramic Society, 40, 211-214.

McMillan, P.F., Wolf, G.H., and Poe, B.T. (1992) Vibrational spectroscopy of silicate liquids and glasses. Chemical Geology, 96, 351-366.

Meade, C., Hemley, R.J., and Mao, H.K. (1992) High-pressure X-ray diffraction of SiO_2 glass. Physical Review Letters, 69, 1387-1390.

Moynihan, C.T., Easteal, A.J., Bolt, M.A., and Tucker, J. (1976) Dependence of the fictive temperature of glass on cooling rate. Journal of the American Ceramic Society, 59, 12-16.

Mysen, B.O., and Frantz, J.D. (1994) Silicate melts at magmatic temperatures: in situ structure determination to 1651^{o}C and effect of temperature and bulk composition on the mixing behavior of structural units. Contributions to Mineralogy and Petrology, 117, 1-14.

Mysen, B., and Richet, P. (2005) Silicate Glasses and Melts, Volume 10: Properties and Structure (Developments in Geochemistry) 1st (first) edition Elsevier Science.

O'Neill, H.S.C., Berry, A.J., McCammon, C.C., Jayasuriya, K.D., Campbell, S.J., and Foran, G. (2006) An experimental determination of the effect of pressure on the $Fe^{3+}/\sum Fe$ ratio of an anhydrous silicate melt to 3.0 GPa. American Mineralogist, 91, 404-412.

Ochs, F.A., and Lange, R.A. (1999) The density of hydrous magmatic liquids. Science, 283, 1314-1317.

Paris, E., Dingwell, D.B., Seifert, F.A., Mottana, A., and Romano, C. (1994) Pressure-induced coordination change of Ti in silicate glass: a XANES study. Physics and Chemistry of Minerals, 21, 510-515.

Richet, P., and Neuville, D.R. (1992) Thermodynamics of silicate melts: Configurational properties. In Thermodynamic data. Springer New York, 132-161.

Richter, D., and Simmons, G. (1974) Thermal-Expansion Behavior of Igneous Rocks. International Journal of Rock Mechanics and Minining Sciences, 11, 403-411.

Sakamaki, T., Ohtani, E., Urakawa, S., Suzuki, A., and Katayama, Y. (2010) Density of dry peridotite magma at high pressure using an X-ray absorption method. American Mineralogist, 95, 144-147.

Sanchez-Valle, C., and Bass, J.D. (2010) Elasticity and pressure-induced structural changes in vitreous $MgSiO_3$-enstatite to lower mantle pressures. Earth and Planetary Science Letters, 295, 523-530.

Sanchez-Valle, C., Chio, C.-H., and Gatta, G.D. (2010) Single crystal elastic properties of $(Cs,Na)AlSi_2O_6.H_2O$ pollucite: a zeolite with potential use for long-term storage of Cs radioisotopes. Journal of Applied Physics, 108, 093509.

Sato, R.K., and Funamori, N. (2008) Sixfold-coordinated amorphous polymorph of SiO_2 under high pressure. Physical Review Letters, 101, 25502.

Seifert, R., Malfait, W.J., Lerch, P., and Sanchez-Valle, C. (2013a) Partial molar volume and compressibility of dissolved CO_2 in glasses with magmatic compositions. Chemical Geology, 358, 119-130.

Seifert, R., Malfait, W.J., Petitgirard, S., and Sanchez-Valle, C. (2013b) Density of phonolitic magmas and time scales of crystal fractionation in magma chambers. Earth and Planetary Science Letters, 381, 12-20.

Shim, S.H., and Catalli, K. (2009) Compositional dependence of structural transition pressures in amorphous phases with mantle-related compositions. Earth and Planetary Science Letters, 283, 174-180.

Stebbins, J.F., Dubinsky, E.V., Kanehashi, K., and Kelsey, K.E. (2008) Temperature effects on non-bridging oxygen and aluminium coordination number in calcium aluminosilicate glasses and melts. Geochimica et Cosmochimica Acta, 72, 910-925.

Stebbins, J.F., and McMillan, P.F. (1989) Five-and six-coordinated Si in $K_2Si_4O_9$ glass quenched from 1.9 GPa and 1200^0C. American Mineralogist, 74, 965-968.

Stebbins, J.F., and Poe, B.T. (1999) Pentacoordinate silicon in high-pressure crystalline and glassy phases of calcium disilicate ($CaSi_2O_5$). Geophysical Research Letters, 26, 1231-1233.

Stebbins, J.F., and Sykes, D. (1990) The structure of $NaAlSi_3O_8$ liquid at high pressure: new constraints from NMR spectroscopy. American Mineralogist, 75, 943-946.

Sykes, D., Poe, B.T., McMillan, P.F., Luth, R.W., and Sato, R.K. (1993) A spectroscopic investigation of anhydrous $KAlSi_3O_8$ and $NaAlSi_3O_8$ glasses quenched from high pressure. Geochimica et Cosmochimica Acta, 57, 1753-1759.

Tkachev, S.N., Manghnani, M.H., Williams, Q., and Ming, L.C. (2005) Compressibility of hydrated and anhydrous Na_2O-SiO_2 liquid and also glass to 8 GPa using Brillouin scattering. Journal of Geophysical Ressearch-Solid Earth, 110 B, 07201.

Tool, A.Q. (1946) Relation between Inelastic Deformability and Thermal Expansion of Glass in Its Annealing Range. Journal of the American Ceramic Society, 29, 240-253.

Velde, B., and Kushiro, I. (1978) Structure of sodium aluminum-silicate melts quenched at high pressure - infrared and aluminum K-radiation data. Earth and Planetary Science Letters, 40, 137-140.

Williams, Q., and Jeanloz, R. (1988) Spectroscopic evidence for pressure-induced coordination changes in silicate glasses and melts. Science, 239, 902-905.

Xue, X.Y., Stebbins, J.F., Kanzaki, M., and Tronnes, R.G. (1989) Silicon coordination and speciation changes in a silicate liquid at high pressures. Science, 245, 962-964.

Xue, X.Y., Stebbins, J.F., Kanzaki, M., McMillan, P.F., and Poe, B. (1991) Pressure-induced silicon coordination and tetrahedra structural changes in alkali oxide-silica melts up to 12 GPa: NMR, Raman, and infrared spectroscopy. American Mineralogist, 76, 8-26.

Xue, X.Y., Stebbins, J.F., and Kanzaki, M. (1994) Correlations between ^{17}O NMR parameters and local structure around oxygen in high-pressure silicates: implications for the structure of silicate melts at high pressure. American Mineralogist, 79, 31-42.

Yamada, A., Gaudio, S.J., and Lesher, C.E. (2010) Densification of $MgSiO_3$ glass with pressure and temperature. Journal of Physics: Conference Series ,215, 012085.

Yarger, J.L., Smith, K.H., Nieman, R.A., Diefenbacher, J., Wolf, G.H., Poe, B.T., and McMillan, P.F. (1995) Al coordination changes in high-pressure aluminosilicate liquids. Science, 270, 1964-1967.

Zha, C.S., Hemley, R.J., Mao, H.K., Duffy, T.S., and Meade, C. (1994) Acoustic velocities and refractive index of SiO_2 glass to 57.5 GPa by Brillouin scattering. Physical Review B, 50, 13105-13112.

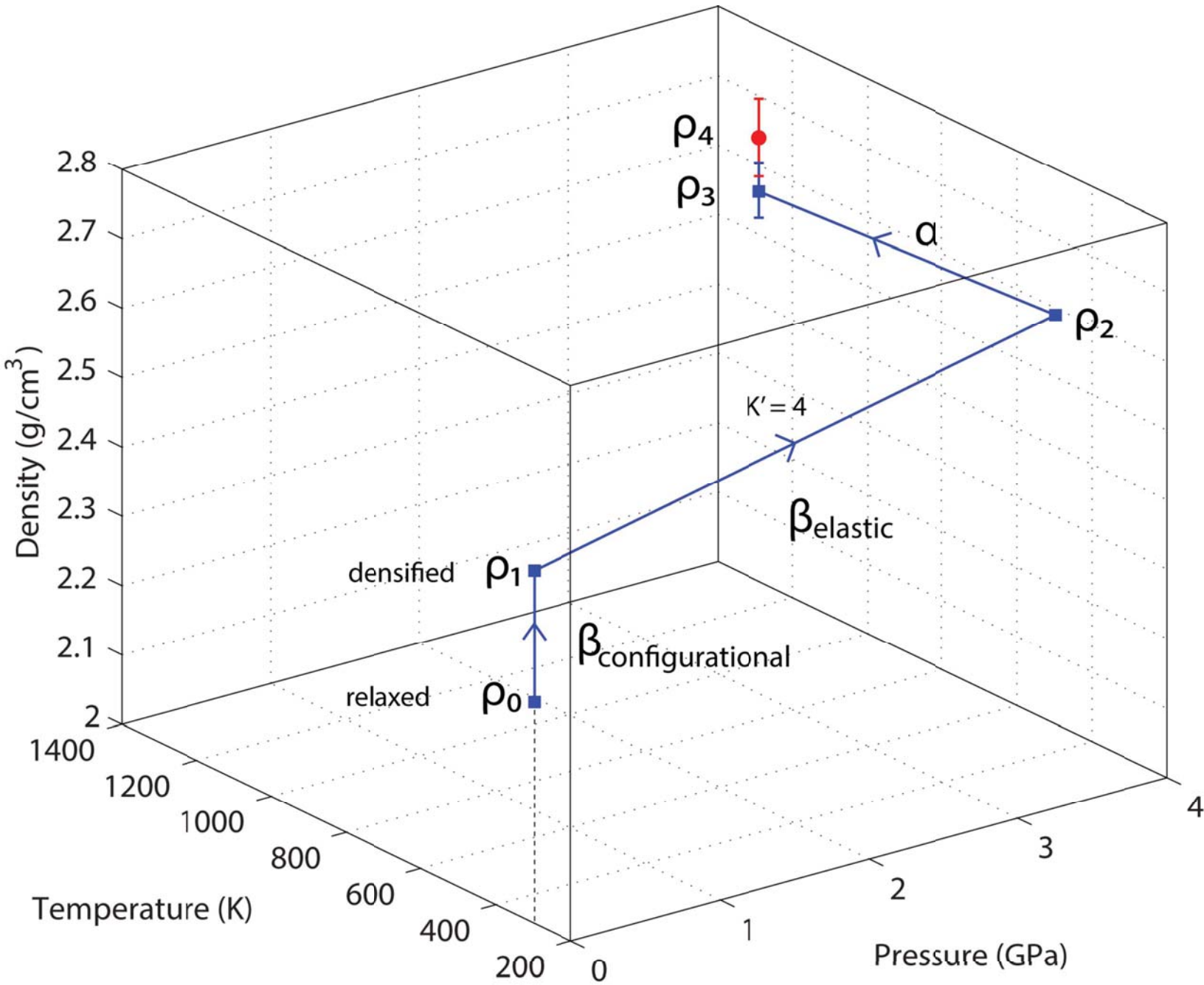
ρ4
ρ3
α
ρ2
K′ = 4
βelastic
densified
ρ1
βconfigurational
relaxed
ρ0
Density (g/cm3)
2.8
2.7
2.6
2.5
2.4
2.3
2.2
2.1
2
1400
1200
1000
800
600
400
200
Temperature (K)
0
1
2
3
4
Pressure (GPa)

Table 1. Compositions (wt%) and synthesis conditions.

	Rhyolite	Phonolite	Basalt
SiO_2	78.5 (4)	56.5 (5)	52.0 (2)
TiO_2	-	0.53 (4)	0.65 (5)
Al_2O_3	12.0 (2)	23.3 (4)	20.2 (2)
FeO	-	-	-
MgO	-	4.0 (1)	11.4 (2)
CaO	-	1.6 (1)	13.2 (1)
Na_2O	4.6 (1)	7.9 (1)	2.3 (1)
K_2O	4.7 (1)	6.1 (1)	-
H_2O [1]	0.32	0.02	0.16
CO_2 [1]	0.00	0.00	0.00
Total	100.12	99.95	99.91
P (GPa)	3.5	2.0	3.5
T (K)	2023	1673	1973
Duration (hrs)	5	2	0.42

[1] FTIR, uncertainty on H_2O and CO_2 is 10% relative, related to uncertainties in the molar absorption coefficients.

Table 2. Volumetric properties.

	Rhyolite	Phonolite	Basalt
Relaxed glasses			
T (K)	298	298	298
P (GPa)	0.0001	0.0001	0.0001
v_P (m/s)	5773 (9)	6040 (15)	6704 (15)
v_S (m/s)	3606 (6)	3594 (10)	3796 (9)
K_S (GPa)	37.1 (5)	47.8 (7)	69.9 (1.1)
ρ_0 (g/cm^3)	2.318 (12)	2.482 (12)	2.717 (14)
V_0/V_0	1	1	1
Permanently densified glasses			
T (K)	298	298	298
P (GPa)	0.0001	0.0001	0.0001
v_P (m/s)	6194 (9)	6220 (11)	6885 (33)
v_S (m/s)	3756 (10)	3664 (6)	3892 (20)
K_S (GPa)	49.1 (6)	53.5 (7)	78.7 (1.1)
ρ_1 (g/cm^3)	2.508 (13)	2.574 (13)	2.892 (14)
V_1/V_0	0.924 (7)	0.964 (7)	0.940 (7)
Densification due to elastic compressibility (K' = 4) [a]			
T (K)	298	298	298
P (GPa)	3.5	2	3.5
ρ_2 (g/cm^3)	2.671 (18)	2.665 (14)	3.013 (16)
V_2/V_0	0.868 (7)	0.931 (7)	0.9018 (7)
Thermal expansion			
T_g (K) [b]	1090	951	947
P (GPa)	3.5	2	3.5
α (10^{-6}/K) [c]	13.3	25.3	15.9
ρ_3 (g/cm^3)	2.643 (30)	2.622 (30)	2.982 (34)
V_3/V_0	0.877 (10)	0.947 (12)	0.911 (11)
Equations of state for silicate melts			
T_g (K) [b]	1090	951	947

P (GPa)	3.5	2	3.5
ρ_4 (g/cm^3)	2.721 (54) [d]	2.692 (54) [e]	3.011 (50) [f]
V_4/V_0	0.852 (18)	0.922 (19)	0.902 (17)

[a] Uncertainties include the results for calculations for K' ranging from 2 to 8.
[b] Giordano et al. (2008).
[c] Ochs and Lange (1999), Bouhifd et al. (2001), Richter and Simmons (1974).
[d] EoS for rhyolitic melts from Malfait et al. (2014).
[e] EoS for phonolitic melts from Seifert et al. (2013).
[f] Multi-component model from Malfait et al. (submitted).